NM WRRI Student Water Research Grant Progress Report Form
Progress Report due Friday October 1, 2021
Draft Final Report due Friday, April 22, 2022
Final Report due Thursday May 19, 2022

1. **Student Researcher:** Ethan Williams (ethan.williams@student.nmt.edu)
   Faculty Advisor: Alex Rinehart (alex.rinehart@nmt.edu)

2. **Project title:**

   Quantifying groundwater to surface water exchanges in the Belen reach of the MRGCD

3. **Description of research problem and research objectives.**

   This study seeks to constrain the volumetric and chemical influence of groundwater on surface water in the southern Albuquerque Basin. Previous work has demonstrated that deep upwelling groundwater is a primary source of Rio Grande salinization (Hogan et al., 2007), but the spatial distribution of these inputs are not well known, nor how the volumetric flow of these inputs change throughout a year. Other groundwater contributions to surface flows (e.g., irrigation returns, lateral basin flowpaths) are also poorly constrained, yet can be assumed to provide a significant component of baseflow as well as the river's solute load. As structural controls force flow paths to converge as they exit the basin, the solute contribution from each distinct source contributes to the chemical evolution of the riparian aquifer and the river itself. Quantifying the proportions of distinct groundwater contributions to the Rio Grande hydrologic system will help evaluate the system's resilience in the face of increased water stress. We consider the chemical, spatial, and temporal variability of groundwater discharge to identify and disaggregate contributions from distinct water sources to understand their individual influence on the riparian system to inform water management decisions, salinization mechanics, and drought resilience

   The objectives of this project are to (1) Identify the proportion and provenance of groundwater contributions in the study area, (2) record how these fluxes change through the 2021 water year, and (3) integrate the results into the hydrogeologic context of the basin. The first and second objectives will be achieved by collecting water samples and flow data at strategic locations in the project area over multiple field campaigns and performing end-member mixing analysis (EMMA). The third objective will be met by presenting our findings in the context of the literature, performing sensitivity analysis, and developing conceptual flow models for the study.

4. Description of methodology employed.

Methods Overview

Five sampling campaigns were preformed in 2021 in the months of March, May, August, October, and December. During each campaign, water samples were collected from the Rio Grande main channel and adjacent riverside drain between Bosque Farms and San Acacia, at approximately 165, 155, 141, 135, 124, and 116 river miles above Elephant Butte. No drain samples were collected at San Acacia (River mile 116). Water samples were analyzed for a suite of geochemical constituents, including major and minor anions and cations, trace metals, $^{87}Sr/^{86}Sr$, $\delta^{18}O$, and $\delta^{2}H$. Field parameters including pH, TDS, specific conductivity, temperature, and dissolved oxygen were measured in site during sample collection with a YSI EXO1 multiprobe. All the geochemical constituents were measured in all samples collected excluding $^{87}Sr/^{86}Sr$, which was only analyzed in the riverside drains and the river at river miles 165 and 116 to conserve costs. Differential flow gauging was performed synchronously to sample collection in the riverside drains using a conventional flow meter as well as dilution gauging with rhodamine dye. Flow data from the river was obtained from data recorded from USGS gauges ISLN5 (river mile 172.5), RGQN5 (river mile 140.8), and SNAN5 (river mile 116). Quantitative provenance analysis was performed using solute and isotope mass balance equations of $^{87}Sr/^{86}Sr$ and Sr^{2+} concentrations using endmember data obtained from Hogan et al. 2007, Burke et al. 1982, and Mukhopadhyay and Brookins 1976.

Water sampling and analysis

Water samples were collected from the drains and river into acid-washed 250ml and 120 ml HDPE bottles using a 'Montana style' peristaltic pump (Woessner, 2007) and an inline 0.45 micron filter. Samples for trace metal and $^{87}Sr/^{86}Sr$ analysis were acidified using trace metal grade nitric acid. $\delta^{18}O$ and $\delta^{2}H$ samples were collected in glass no-headspace vials directly from the channel. Samples were refrigerated upon collection until analysis. In some instances, flow in the Rio Grande was too turbid to effectively filter in the field. In those cases, grab samples were collected directly from the river and were frozen prior to filtration in the laboratory. Cations, anions, and trace metals were analyzed in the New Mexico Bureau of Geology Analytical Chemistry Laboratory using EPA methods 200.7, 300.0, and 200.8 respectively by the grant recipient with assistance from laboratory personnel. $\delta^{18}O$ and $\delta^{2}H$ were also analyzed at the Bureau using a Picarro isotope analyzer with assistance from Bureau staff. $^{87}Sr/^{86}Sr$ analysis was conducted at the University of Texas at El Paso with a Nu Plasma HR multi-collector ICP-MS by Dr. Lin Ma and his supervisees.

Flow Gauging

Differential flow gauging was performed in drains using conventional and dilution methods in the interest of redundancy and accuracy. Differential flow gauging accounts for gains or losses in flow volume over distance due to groundwater flux, and is simply the difference between the downstream and upstream discharges divided by the interval between

measurements. Measurement intervals used in the drains spanned from 188 to 800 meters; greater spacing was used for sites with higher flow volumes. Conventional flow gauging was performed using a Hach model FH950.0 flow meter and wading rod using standard methods (ISO 748-2021). Average velocity ($\overline{v}$) was recorded using the one-point method, where velocity is measured at 0.6 of total depth (d) below surface. Readings were taken at one-foot intervals across the channel. Total discharge (Q) was calculated using the mid-section method, where total discharge is given by equation 1, in which n= measurement number, m= number of measurements, and b = the distance of a measurement from bank.

$$Q = \sum_{n=1}^{m} \overline{v_n} \, d_n \left(\frac{b_{n+1} - b_{n-1}}{2} \right) \tag{1}$$

Dilution flow gauging was performed using the slug-injection method outlined by Kilpatrick and Cobb (1985). Rhodamine wt fluorescent dye was used as the tracer and was measured in situ by Turner C3 fluorometers. These instruments have rhodamine wt specific optical sensors and were calibrated prior to deployment to measure rhodamine concentration based on relative fluorescence. Dye was injected into the channel upstream of the measurement interval at a distance sufficient for complete longitudinal mixing to occur, and the passage of the dye plume was recorded at 10 second intervals by fluorometers placed at each end of the measurement interval. Discharge at each location was calculated by dividing the amount of dye injected by the area of the time concentration curve recorded by each flurometer per equation 2, where S_G= the dye's specific gravity, V_I= the volume of dye injected, C= the concentration of the dye, and A_c= the area under the time concentration curve.

$$Q = \frac{S_G V_I C}{A_c} \tag{2}$$

Geochemical analysis

Mixing behavior was evaluated using multiple lines of evidence including simple solute-solute plots, $\delta^{18}O$ vs. δ^2H, (CO_3^{2-} +HCO_3^-)-(SO_4^{2-} +Cl^-) vs. (Ca^{2+}+Mg^{2+})-(Na^++K^+), endmember mixing analysis (EMMA), as well as $^{87}Sr/^{86}Sr$ and Sr^{2+} solute and isotope mass balance equations. Chemical variability was compared against spatial distribution and the composition of potential endmembers, such as groundwaters from hydrogeochemical zones identified by Plummer et al. (2004) and deep basin brine (Hogan et al. 2007; Williams et al. 2013).

EMMA was performed following the procedure of Christophersen and Hooper (1992). Principal component analysis was done in RStudio on geochemical species that exhibited some conservative mixing behavior (as evidenced by a high correlation coefficient between two solutes) using the 'prcomp' function. This function normalizes and centers the data then uses a singular value decomposition to identify vectors corresponding to maximums in the sample dataset's variance. These vectors are referred to principal components and are used as axes in a new Euclidian space in which the input data and potential endmembers are transposed. The number of endmembers required to describe the mixing behavior of the n+1, where n is the number of principal components that describe a significant component of the total variance.

Endmember identification can be performed in mixing space, where valid endmembers should circumscribe the data. Mixing calculations can then be performed based on the Euclidean distance between samples and endmembers in principal component space. Successful EMMA requires true conservative mixing behavior from the input species and sufficiently extreme endmember compositions to isolate mixing processes from nonconservative processes like mineral dissolution, redox, or cation exchange. Including nonconservative species (e.g. major cations) into the principal component analysis disqualifies mixing calculations but helps to identify notable geochemical processes that are controlling the system.

Mixing calculations using solute and isotope mass balance equations of $^{87}Sr/^{86}Sr$ and Sr^{2+} concentrations were performed following the procedure for three-component mixing described by Clark (2015, pg. 157). This approach was chosen due to the distribution of data in $^{87}Sr/^{86}Sr$ vs. $1/[Sr^{2+}]$ plots, wherein observations could be circumscribed by three endmembers including Rio Grande headwater flows ($[Sr^{2+}] \cong 0.25ppm$, $^{87}Sr/^{86}Sr \cong 0.7906$), Sedimentary brine flows ($[Sr^{2+}] \cong 10.6$ ppm, $^{87}Sr/^{86}Sr \cong 0.7106$), and water influenced by Paleozoic sediment ($[Sr^{2+}] \cong 3$ ppm, $^{87}Sr/^{86}Sr \cong 0.7090$) (Hogan et al., 2007; Burke et al., 1982; Mukhopadhyay and Brookins, 1976; Plummer et al., 2004). These endmembers made physical sense in the context of the hydrologic system, as samples collected near regions with high Paleozoic sediment fractions plotted towards the Paleozoic endmember, and samples collected where basin geometry supports a vertical component of flow plotted towards the brine endmember. The system of equations used to solve for endmember fractions is given in equations 3, 4, and 5, where m = the mass of Sr^{2+}, δ = the $^{87}Sr/^{86}Sr$ value, and f = endmember fraction.

$$f_{Brine} = \frac{m_{Sample} - m_{Rio} - f_{Paleo}(m_{paleo} - m_{Rio})}{m_{Brine} - m_{Rio}} \qquad (3)$$

$$f_{Rio} = \frac{\delta_{Sample} m_{Sample} - \delta_{Brine} m_{Brine} - f_{paleo}(\delta_{Paleo} m_{Paleo} - \delta_{Brine} m_{Brine})}{\delta_{Rio} m_{Rio} - \delta_{Brine} m_{Brine}} \qquad (4)$$

$$f_{Paleo} = 1 - f_{Brine} - f_{Rio} \qquad (5)$$

5. Description of results; include findings, conclusions, and recommendations for further research.

Results Summary

Our investigation yielded insight into the timing, distribution, and mechanics of interactions between groundwater and surface water in the southern Albuquerque Basin. $^{87}Sr/^{86}Sr$ data collected from March and May are consistent with three system endmembers: Rio Grande through-flow ($^{87}Sr/^{86}Sr = 0.7096$), upwelling sedimentary brine ($^{87}Sr/^{86}Sr \geq 0.7106$), and water influenced by Paleozoic sediment ($^{87}Sr/^{86}Sr = 0.7090$). Preliminary end-member mixing analysis indicates one or more additional end-member waters could be present. Strontium isotope mass balance showed that sedimentary brine and Paleozoic-influenced water

accounted for as much as 5% and 11% of drain flow respectively. The greatest net increase in the Rio Grande's salinity throughout the project area was observed in March, where Cl^- concentration increased from 21.2 to 50.5 mg/l throughout the project area and $^{87}Sr/^{86}Sr$ increased from 0.70955±0.00016 to 0.70996±0.00003, indicating composition of 2% Paleozoic-influenced water, 2% brine, and 96% Rio Grande throughflow. Groundwater flux measurements ranged from -13.1 to 21.0 $m^3/day/m$ (4.2 $m^3/day/m$ average). Notable trends in water evolution include increases in specific conductance and a transition from a Ca-HCO_3^- towards a Na-HCO_3^- water type. The rate of change increases with proximity to the basin's terminus. $^{87}Sr/^{86}Sr$ in samples from near sub-basin structural highs showed locally elevated brine fractions, inconsistent with the general trend. Increases in Na^+/Ca^{2+} did not always correspond to increases in Cl^-, suggesting cation exchange and water mixing have independent influence. These results demonstrate that shallow lateral groundwater flows are a primary source of salinization in addition to upwelling brine.

Endmember Identification and Mixing Analysis

The hydrologic complexity of the southern Albuquerque Basin presented a challenge for endmember identification using EMMA, as many of the hydrogeochemically distinct groundwaters that potentially interact with the riparian system do not have sufficiently extreme compositions of available conservative chemical constituents to be reliably differentiated (e.g. Central or East Mountain hydrogeochemical zones (Plummer et al. 2004)). EMMA attempts using different combinations of input data consistently indicated that at least four endmembers were needed to adequately describe the mixing system, wherein it is difficult to identify endmembers with reasonable certainty. EMMA investigations are ongoing and may be more successful if: applied selectively to data in spatially similar sample locations; using different normalization schemes; or if more conservative tracers are measured.

Endmember identification and mixing analysis using strontium isotopes yielded promising results. $^{87}Sr/^{86}Sr$ is a particularly valuable tracers for distinguishing water provenance in the Albuquerque basin because (1) $^{87}Sr/^{86}Sr$ is not affected by fractionation or mineral precipitation (Frost and Toner, 2004), (2) carbonate and granitic aquifers have distinct $^{87}Sr/^{86}Sr$ values and can therefore be used to identify origins of salinity (Clark and Fritz, 1997), and (3) previous studies have provided measurements and estimation of $^{87}Sr/^{86}Sr$ values and Sr concentrations of the Rio Grande headwaters and saline waters of the Albuquerque Basin (Hogan et al., 2007; Williams et al., 2013; Mukhopadhyay and Brookins, 1976; Plummer et al., 2004). Salinity in the basin is derived from three primary sources: sedimentary brines that have long resonance times and inherit solute from prolonged mineral interactions (Hogan et al., 2007), interactions with Paleozoic and Mesozoic carbonate and evaporite rock units that exposed at the rift flanks and locally contribute to rift fill material, and endogenic fluids that ascend along fault systems (Williams et al., 2013). Although endogenic fluids have a high initial $^{87}Sr/^{86}Sr$ signature, that value can assimilate to a low carbonate or basaltic signature during water rock interactions during ascension, as apparent in the San Acacia spring system. Headwater derived flows of in the Rio Grande have low Sr content and a moderate $^{87}Sr/^{86}Sr$ value, thus the river, sedimentary brine, and Paleozoic-influenced saline waters can be readily

differentiated using a solute and isotope mass balance three component mixing approach (Clark, 2015). Results from May and March are shown below in figure 1 and table 1. Data from August, October, and December is awaiting analysis at UTEP. The highest brine fractions were observed at river mile (RM) 141, which is possible attribute to a local shallowing in basin depth that aligns with the hydraulic gradient (Grauch and Connell, 2013; Bexfield and Anderholm, 2000). The highest Paleozoic fractions were observed at RM 124, where a Paleozoic sediment is locally abundant in part due to the Rio Puerco. Significant increases of sedimentary brine and Paleozoic influenced waters were recorded between RM 165 and RM 116 in March, where river salinization was also significant. This was not seen in May, likely due to high spring runoff.
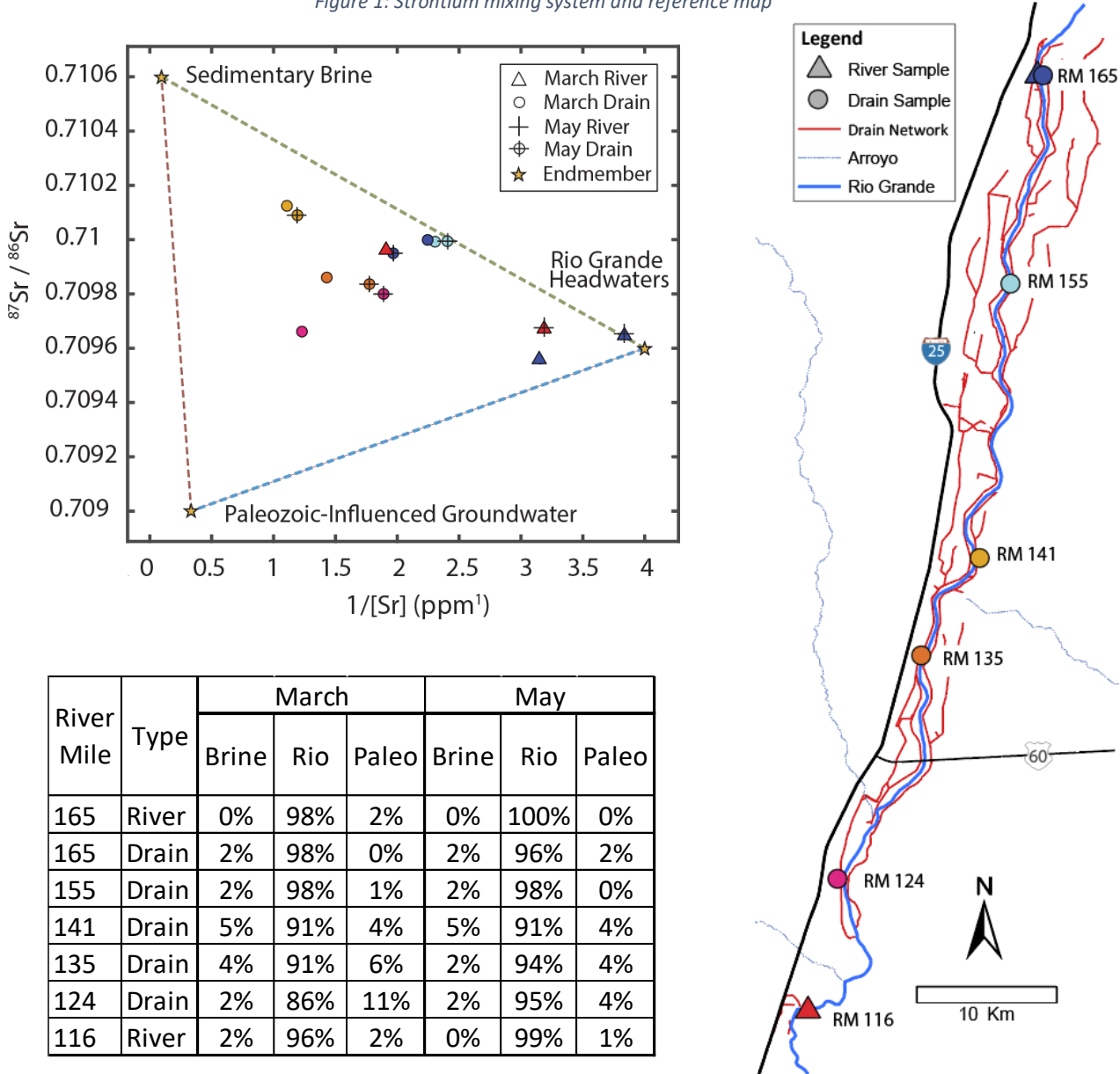
Figure 1: Strontium mixing system and reference map

River Mile	Type	March			May		
		Brine	Rio	Paleo	Brine	Rio	Paleo
165	River	0%	98%	2%	0%	100%	0%
165	Drain	2%	98%	0%	2%	96%	2%
155	Drain	2%	98%	1%	2%	98%	0%
141	Drain	5%	91%	4%	5%	91%	4%
135	Drain	4%	91%	6%	2%	94%	4%
124	Drain	2%	86%	11%	2%	95%	4%
116	River	2%	96%	2%	0%	99%	1%

Table 1: Mixing fractions determined from Sr isotope mass balance

Flow Gauging

Results of differential flow gauging performed using a conventional flow meter at drain sites are given in table 2. These results are indicative of local flux conditions in the vicinity of sample locations. Dilution gauging performed synchronous to conventional gauging had poor agreement to conventional gauging. Disparity between conventional and dilution discharge measurements increased in with high turbidity flow conditions suggesting that the rhodamine wt dye tracer used for dilution gauging was prone to sorbing to suspended sediment, resulting in incomplete recovery of the tracer at measurement sites which renders the dilution method invalid. We have a high degree of confidence in the accuracy of conventional gauge measurements due to the near ideal drain channel geometries, which encourage laminar flow and convenient measurements. However, manual gauge measurements could not always be collected due extensive channel vegetation or dangerously high flows.

Weekly average river discharge from USGS gauges ISLN5 (river mile 172.5), RGQN5 (river mile 140.8), and SNAN5 (river mile 116) are presented in figure 2, which highlights the overall flow dynamics of the system throughout 2021. In winter and early spring, flow volumes increased throughout the project area indicating a gaining system. This pattern was reversed following runoff, where significant flow loss between ISLN5 and RGQN5 was recorded. Minimal losses, if any, were observed between RGQN5 and SNAN5 and may be due in part to open water evaporation.

Figure 2: Weekly average river discharges in 2021 and timing of sampling campaigns. Missing data may be due to gauge maintenance, database issues, or recording issues. ISLN5 readings are corrected for diversions directly below the gauge location based off of MRGCD gauge data in order to provide an true assessment of river flow.
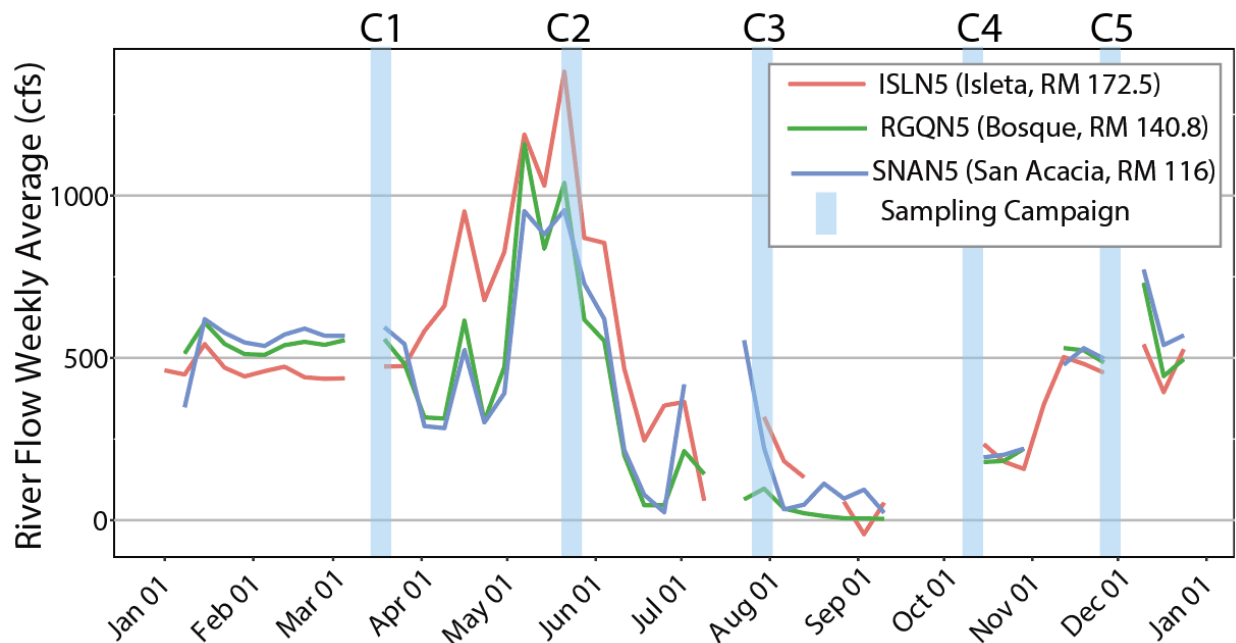
Table 2: Manual gauge measurements and groundwater flux rates. Data gaps are due to the inability to preform measurements due to disadvantageous flow conditions or extensive channel vegetation.

Drain Site	Campaign	Q (cfs) up-stream	Q (cfs) down-stream	Avg. Q (cfs)	Avg. Q (m³/s)	Calculated Flux (m³/d/m)	% Change per 100m
RM 165	March						
RM 155		43.5	43.9	43.7	12.4	3.5	0.3
RM 141							
RM 135		14.9		14.9	4.2		
RM 124		33.4	35.3	34.4	9.7	23.0	2.8
RM 165	May			12.9	3.6		
RM 155		29.1	33.8	31.5	8.9	14.4	2.0
RM 141		4.9	6.0	5.5	1.5	13.1	10.9
RM 135		52.5	51.5	52.0	14.7	-13.1	-1.0
RM 124		64.2	63.1	63.7	18.0	-4.3	-0.3
RM 165	August						
RM 155		41.0	43.9	42.4	12.0	9.1	0.9
RM 141		2.1	2.7	2.4	0.7	7.7	15.1
RM 135		79.8	79.8	79.8	22.6	-0.5	0.0
RM 124		57.6	62.3	59.9	17.0	17.3	1.2
RM 165	October	20.1	18.8	19.4	5.5	-8.4	-1.7
RM 155		47.4	47.3	47.4	13.4	-0.3	0.0
RM 141		0.4	0.4	0.4	0.1	0.0	0.0
RM 135		67.2	67.0	67.1	19.0	-2.6	-0.2
RM 124		39.0	40.6	39.8	11.3	5.9	0.6
RM 165	December	7.0	7.4	7.2	2.0	2.5	1.5
RM 155		45.0	46.4	45.7	12.9	4.2	0.4
RM 141			2.4	2.4	0.7		
RM 135		28.6	28.3	28.4	8.0	-3.5	-0.5
RM 124		12.9	16.1	14.5	4.1	11.7	3.7

Chemical Evolution and Salinization

Salinity and overall solute load generally increased with flow distance, but the range and magnitude of increase varied significantly across measurement campaigns. Using chloride as a proxy for total salinity, we observed a significant (138%) increase in March, a moderate (46%) increase in August, increases of 20-22% in December and May, and a 3% decrease in October (figure 3). The October decrease is likely due to less saline irrigation return flows from early in

the season entering the river and diluting river flows which by this point in the season were being fed from an evaporated source, which is supported by a heavier isotopic composition of water at north end of the project area and similar major ion compositions between the river and drains (figure 8).

During all campaigns, drain water demonstrated an increase in sodium relative to calcium, and chloride and sulphate relative to alkalinity with flow distance. This trend was also observed in the river, except for May where minimal changes in major ions were observed (figure 6). Trends in cation concentration are interpreted to be driven by cation exchange and mineral precipitation in addition to mixing with sodic groundwater. River samples from December were dominantly sodic and highly variable. These samples were collected unfiltered from the river and frozen prior to lab filtration and subsequent analysis, which may have allowed for cation exchange to occur in the sample bottles despite being frozen. The freezing method was employed for the sake of convenience and sampling efficiency on the premise that equilibration with sediments would be kinetically unfavorable in a frozen matrix. Another explanation is a complicated mix of highly evolved irrigation return flows were flushing out of the system while regional groundwater flow patterns were becoming reestablished. This possibility is supported by the composition of the RM 124 (La Joya) drain, which shifted to a sodium chloride water type during this month perhaps due to in part evaporated ponded water in the adjacent Bernardo Waterfowl Management area or high volumes of saline groundwater. Abnormalities are not observed in the other drains in December – and all December drains were collected using standard practices.

Assuming the 138% increase in river chloride concentration recorded in March is completely attributable to the 4% gross contributions from sedimentary brine (2%) and Paleozoic influence saline waters (2%) as determined from strontium isotope analysis, the average chloride concentration of those waters would be 730 ppm. This is in the range of the Western Boundary hydrogeochemical groundwater zone identified by Plummer et al., 2004 (820 ppm) which can be assumed to have a Paleozoic Sr signature. Hogan et al. (2007) estimated that basin brines have a chloride concentration of 1000 ppm, which is in the range of brine composition determined by mass balance calculations from the RM 141 (Bosque) drain based the mixing fractions indicated by Sr isotope analysis (1080 ppm in May). The Rio Puerco hydrogeochemical zone has an average chloride concentration of 185 ppm (Plummer et al., 2004) and San Acacia endogenic spring waters have variable chloride concentrations of over 5000 ppm and have an intermediate Sr signature of ~0.70975 (Williams et al., 2013). Assuming sedimentary brine compositions are 1000 ppm, average Paleozoic-influenced waters should have a chloride concentration of ~500 ppm according to mass balance calculations using march data. This value is consistent with a mixture of groundwaters from the Western Boundary and Rio Puerco hydrogeochemical zones.

During the march campaign, volumetric flow in the river increased by more than 4% between the Isleta and San Acacia River gauges. This implies that additional sources of groundwater contributed to river flow. These may include Central, West Central, or East Mountain hydrogeochemical groundwater zones which all have chloride concentrations under 20 ppm (Plummer et al., 2004). During baseflow conditions, it is reasonable to conclude that a combination of these sources are the primary source of volumetric groundwater contributions but have negligible impact on salinization. Irrigation return flows are another potential salinity source. The RM 165 river sample had a chloride concentration of 37.3 ppm, and is a reasonable proxy for the maximum salinity of waters diverted into the Belen irrigation district. Assuming a worst-case scenario where irrigation waters with 40 ppm chloride are evaporated by 75% at or near the surface, return flow chloride concentration could be as high as 160 ppm. However, it is unlikely that volumetrically significant return flows would be present half a year after the end of irrigation season. The impact of irrigation return flows can be assumed to be greatest during and immediately after irrigation season, such as during the August and October measurement campaigns. Chloride accumulation in the river was minimal during these campaigns, and dramatic increases in drain chloride concentrations were not observed. Overall chloride concentrations were typically higher during these months (as well as December) and δ^{18}O & δ^2H values were elevated (particularly in October) suggesting that open water evaporation and return flows of evaporated irrigation water do increase salinity but only to a moderate extent.

Figure 3: Chloride concentration with flow distance. The closest towns to sample locations are noted at the top.
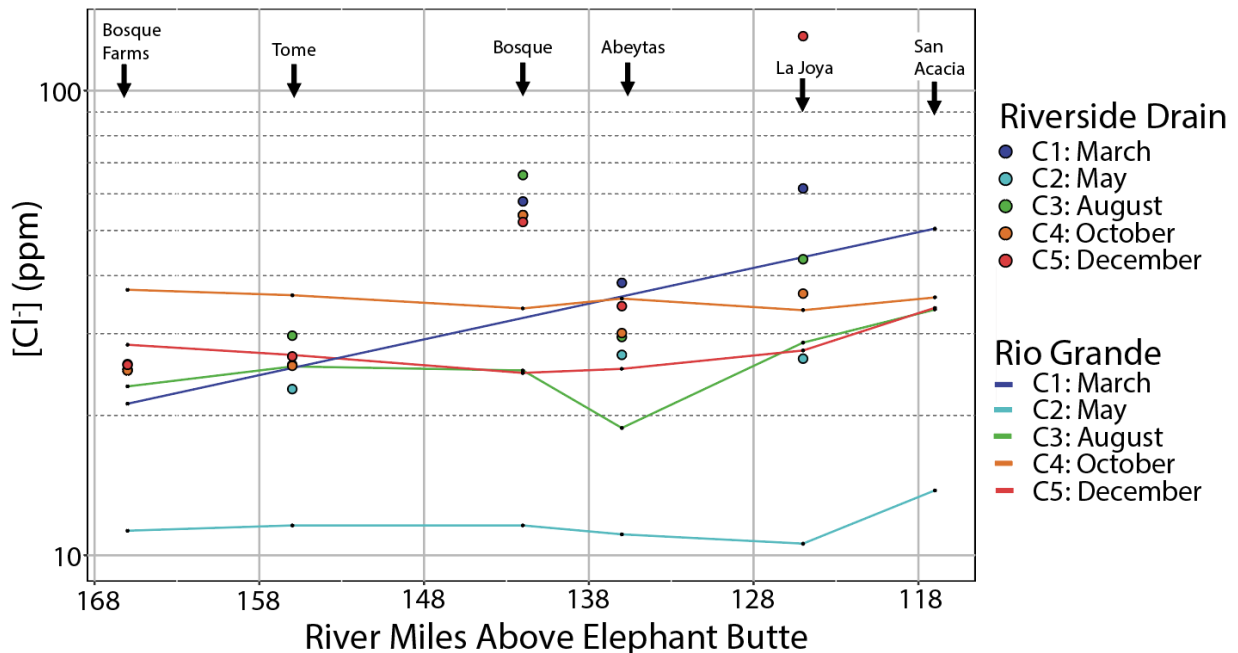
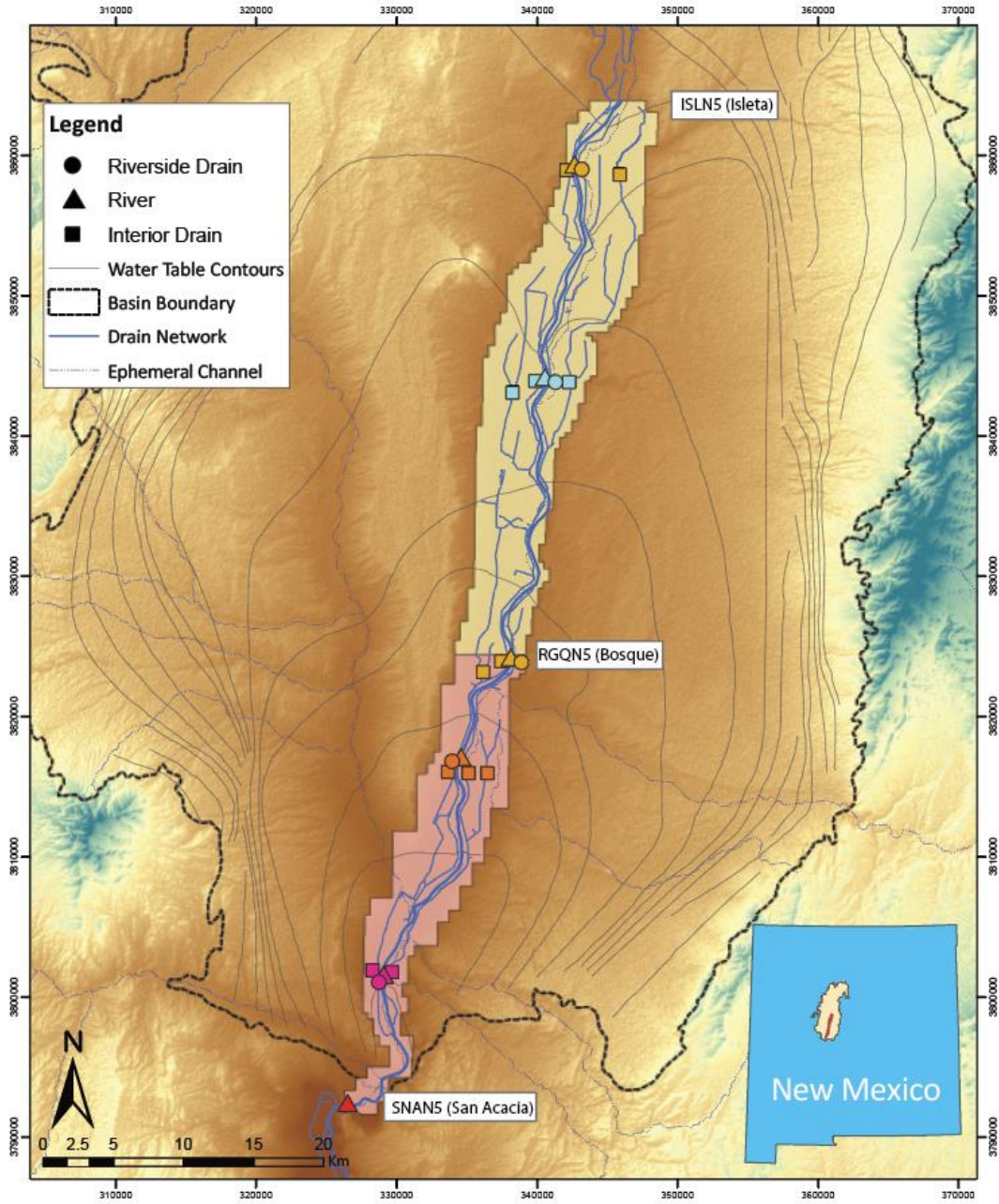*Figure 4: Project area overview and symbol key for figures 4 through 9*
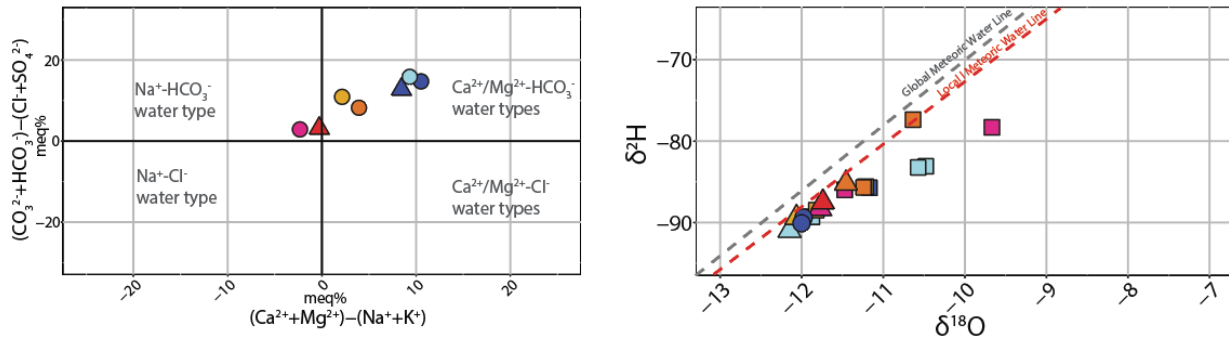

Figure 5: March trends in major ions and δ18O vs. δ2H

Figure 6: May trends in major ions and δ18O vs. δ2H

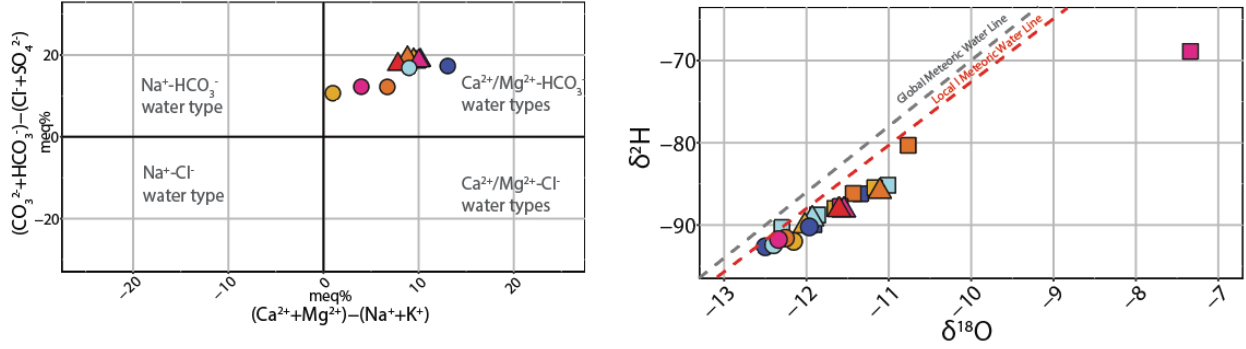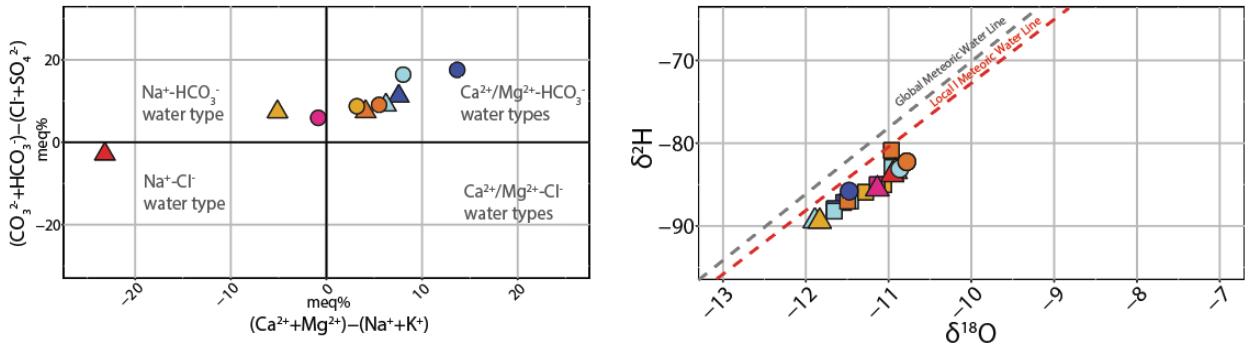Figure 7: August trends in major ions and δ18O vs. δ2H
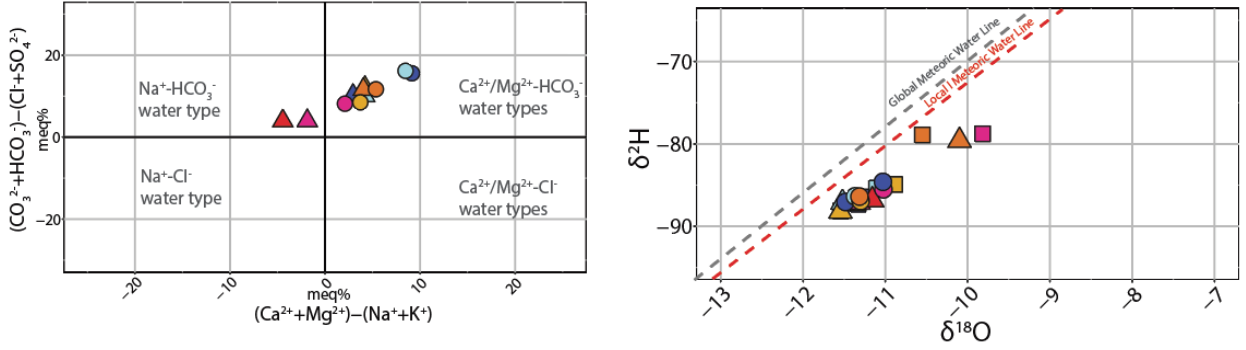

Figure 8: October trends in major ions and δ18O vs. δ2H
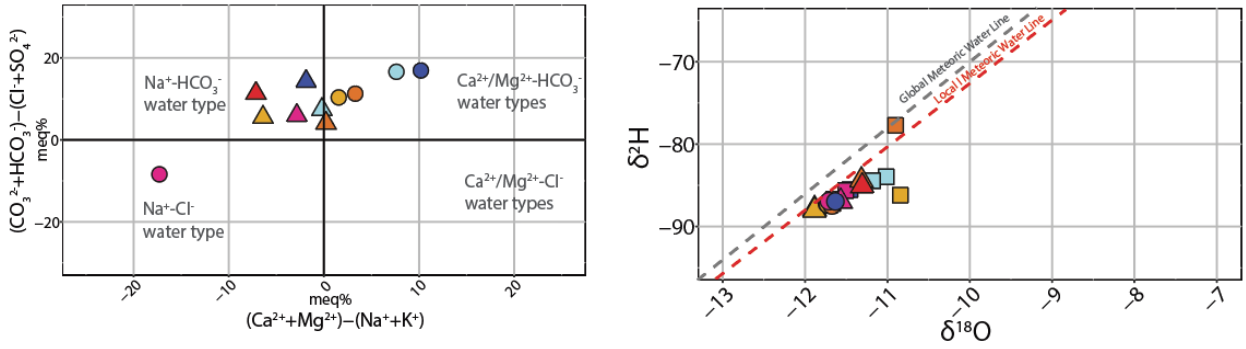

Figure 9: December trends in major ions and δ18O vs. δ2H

6. **Provide a paragraph on who will benefit from your research results. Include any water agency that could use your results.**

These results may benefit future researchers and New Mexico water managers, including the Middle Rio Grande Conservancy District, Interstate Stream Commission, and the Bureau of Reclamation. The main takeaway for water managers is that groundwater is responsible for the bulk salinity increases that occur in the Albuquerque Basin and are most significant during baseflow conditions. During drought, saline groundwater will likely account for a greater proportion of river flows and salinization risk will increase. The Rio Grande is a generally gaining river between river mile 141 and 116. Drying risk is low but salinization risk is high in that interval. Salinization risk and river solute concentrations are lowest during spring runoff; maximizing deliveries to downstream reservoirs during this period would reduce reservoir salinization caused by evaporative concentration.

7. **Describe how you have spent your grant funds. Also provide your budget balance and how you will use any remaining funds. If you anticipate any funds remaining after May 19, 2022, please contact Carolina Mijares immediately. (575-646-7991; mijares@nmsu.edu)**

Our budget balance is zero, all funds will be spent before May 19th, 2022. The majority of funds were allocated towards analytical costs at the NMBGMR ($2,346.00) and UTEP ($4,980.60). Funds were also used to purchase rhodamine wt dye from Turner Designs Inc. ($291.00) as well as miscellaneous equipment and supplies.

8. **List presentations you have made related to the project.**

- Poster Session; Geological Society of America Connects 2021 Conference in Portland, OR; October 11th, 2021

- Oral Presentation; New Mexico Bureau of Geology and Mineral Resources Aquifer Mapping Program (AMP) Seminar Series; October 22, 2021

- Poster Session; NM WRRI 66th Annual New Mexico Water Conference; October 28, 2021

- Poster Session; New Mexico Geological Society 2022 Annual Spring Meeting; April 8, 2022

- Poster Session; 2022 N4WPP Water Symposium; April 23, 2022

9. **List publications or reports, if any, that you are preparing. For all publications/reports and posters resulting from this award, please attribute the funding to NM WRRI and the New Mexico State Legislature by including the account number: NMWRRI-SG-2021.**

   A masters thesis is being prepared based off of the work made in possible in part by this award. Additionally, we plan seek publication in a relevant academic journal in the near future.

10. **List any other students or faculty members who have assisted you with your project.**

    Danial Cadol; associate professor; Department Earth and Environmental Science Department; New Mexico Tech; (daniel.cadol@nmt.edu)

    Lin Ma; associate professor; Earth, Environmental and Resource Sciences Department; University of Texas at El Paso; (lma@utep.edu)

11. **Provide special recognition awards or notable achievements as a result of the research including any publicity such as newspaper articles, or similar.**

    New Mexico Geologic Society Spring Meeting 2022 Best Student Poster Award

12. **Provide information on degree completion and future career plans. Funding for student grants comes from the New Mexico Legislature and legislators are interested in whether recipients of these grants go on to complete academic degrees and work in a water-related field in New Mexico or elsewhere.**

    I plan to prepare and defend my thesis in the coming months and pursue a career as a water science professional in New Mexico. I intend to pursue positions related to hydrogeology and hydrogeochemistry that allow me to continue face challenges in developing and managing our states water resources

References

Burke, W.H., Denison, R.E., Hetherington, E.A., Koepnick, R.B., Nelson, H.F., Otto, J.B., 1982. Variation of seawater 87Sr/86Sr throughout Phanerozoic time. Geol 10, 516. https://doi.org/10.1130/0091-7613(1982)10<516:VOSSTP>2.0.CO;2

Bexfield, L.M., and Anderholm, S.K., 2000, Predevelopment water-level map of the Santa Fe Group aquifer system in the middle Rio Grande basin between Cochiti Lake and San Acacia, New Mexico: U.S. Geological Survey Water-Resources Investigations Report 00–4249, 1 sheet, https://doi.org/10.3133/wri004249.

Christophersen, N., Hooper, R.P., 1992. Multivariate analysis of stream water chemical data: The use of principal components analysis for the end-member mixing problem. Water Resour. Res. 28, 99–107. https://doi.org/10.1029/91WR02518

Clark, I., 2015. Groundwater Geochemistry and Isotopes 442.

Clark, I.D., Fritz, P., 1997. Environmental isotopes in hydrogeology. CRC Press/Lewis Publishers, Boca Raton, FL.

Frost, C.D., Toner, R.N., 2004. Strontium Isotopic Identification of Water-Rock Interaction and Ground Water Mixing. Ground Water 42, 418–432. https://doi.org/10.1111/j.1745-6584.2004.tb02689.x

Geochemical characterization of ground-water flow in the Santa Fe Group aquifer system, Middle Rio Grande Basin, New Mexico, 2004. https://doi.org/10.3133/wri034131

Grauch, V.J.S., Connell, S.D., 2013. New perspectives on the geometry of the Albuquerque Basin, Rio Grande rift, New Mexico: Insights from geophysical models of rift-fill thickness, in: New Perspectives on Rio Grande Rift Basins: From Tectonics to Groundwater. Geological Society of America. https://doi.org/10.1130/2013.2494(16)

Kilpatrick, A., Cobb, E.D., n.d. l MEASUREMENT OF DISCHARGE USING TRACERS 63.

Mukhopadhyay, B., Brookins, D.G., 1976. Strontium isotopic composition of the Madera Formation (Pennsylvanian) near Albuquerque, New Mexico. Geochimica et Cosmochimica Acta 40, 611–616. https://doi.org/10.1016/0016-7037(76)90107-1

Williams, A.J., Crossey, L.J., Karlstrom, K.E., Newell, D., Person, M., Woolsey, E., 2013. Hydrogeochemistry of the Middle Rio Grande aquifer system — Fluid mixing and salinization of the Rio Grande due to fault inputs. Chemical Geology 351, 281–298. https://doi.org/10.1016/j.chemgeo.2013.05.029

Woessner, W.W., 2007. Building a Compact, Low-Cost, and Portable Peristaltic Sampling Pump. Ground Water 45, 795–797. https://doi.org/10.1111/j.1745-6584.2007.00346.x